FOREX Publication
Open Access | Rapid and quality publishing

International Journal of
Electrical and Electronics Research (IJEER)
Research Article | Volume 14, Issue 1| Pages 186-199|e-ISSN: 2347-470X

Sailfish-Optimized Feed Forward Neural Network for Accurate Forecasting and Economic Optimization of Microgrid Energy Systems

Anish Vora[1*], and Rajendragiri Aparnathi[2]

[1]Ph. D. Research Scholar, Department of Electrical Engineering, Faculty of Engineering & Technology, Gokul Global University, Gujarat, India; Email: voraanish@yahoo.com
[2]Professor (Associate), Department of Electrical Engineering, Faculty of Engineering & Technology, Gokul Global University, Gujarat, India; Email: rajendraaparnathi@gmail.com

***Correspondence:** *Anish Vora; anishvoraanish89@gmail.com*

ABSTRACT- The integration of renewable energy sources (RES) such as solar and wind into microgrids introduces challenges in energy balance, voltage stability, and economic dispatch due to their intermittent and variable nature. This paper proposes a novel Sailfish-optimized Feed Forward Neural Network (SbFNN) framework to address these challenges by combining intelligent forecasting with optimization-driven energy management. The FFNN predicts microgrid load, solar, and wind generation, while the Sailfish Optimization algorithm adaptively tunes network weights and minimizes operational costs. The proposed SbFNN improves load balancing, reduces energy losses, and maintains reliable voltage and frequency under varying load conditions. Extensive simulation using a one-year hourly microgrid dataset demonstrates that SbFNN achieves superior forecasting accuracy ($R^2 = 0.993$, MAPE = 0.0093) and statistically significant improvements over benchmark methods. Economic dispatch results show reduced total operating costs and efficient utilization of renewable resources. The SbFNN framework thus offers an effective, adaptive, and scalable solution for future sustainable microgrid management.

Keywords: Microgrid, Sailfish, Cost, Economic Dispatch, Forecasting, Solar, Wind, Load, Feed Forward Neural Network.

ARTICLE INFORMATION

Author(s): Anish Vora, Rajendragiri Aparnathi;
Received: 13/11/2025; **Accepted**: 10/02/2026; **Published**: 30/03/2026;
E- ISSN: 2347-470X;
Paper Id: IJEER1311A10
Citation: 10.37391/ijeer.140120
Webpage-link:
https://ijeer.forexjournal.co.in/archive/volume-14/ijeer-140120.html

Publisher's Note: FOREX Publication stays neutral with regard to jurisdictional claims in Published maps and institutional affiliations.

1. INTRODUCTION

An MG is a modest energy system that works both separately and in combination with the larger power grid. It comprises loads, energy management systems (EMS), and dispersed energy resources [1]. MGs enable the integration of RES, improve energy resiliency, and lessen dependency on centralized power sources [2]. They are beneficial for promoting environmental objectives, in distant locations, and during grid disruptions [3]. In addition to reducing expenses and increasing energy efficiency, microgrid contributes to the development of a more flexible and decentralized energy system [4]. Artificial intelligence (AI) and advanced power electronics have taken control of electrical grids, and this trend might last for many years [5]. The use of advanced AI techniques in MG controls is growing significantly. It provides enhanced transient stability of the power system [6], simple integration and disconnection of distributed generation (DG), and improved power quality for end users [7]. Modern Microgrids depend significantly on distributed energy resources (DERs), which enable localized energy generation and consumption [8]. Advanced management systems are required to effectively integrate these diverse resources [9], and AI is emerging as an essential tool in this sector [10]. AI algorithms evaluate real-time information from multiple sources to enhance decision-making, forecast demand, and supply patterns, and optimize energy distribution [11]. Additionally, AI enables autonomous control systems to adapt to grid conditions in real time, minimizing overloads and improving resilience [12]. Microgrids with DERs can improve efficiency, sustainability, and dependability by leveraging AI.

Artificial intelligence (AI)-enhanced DER integration into Microgrids provides multiple benefits. AI-driven approaches maximize energy production, delivery, and storage, boosting efficiency and decreasing waste [13]. Better resource utilization is ensured by accurate predictions of energy demand and generation from renewable sources, enabled by real-time AI-driven analytics [14]. Since AI responds rapidly to changes or disruptions in the energy supply, this improves Microgrids' resilience and dependability [15]. AI also assists with DER predictive maintenance, reducing operating expenses and downtime [16]. It makes it easier to include renewable energy sources, which contribute to sustainability goals and reduce carbon emissions [17]. Overall, AI improves the efficiency, flexibility, and economic viability of DER-powered microgrids. Nevertheless, there are several drawbacks to employing AI to integrate DERs in Microgrids. High initial costs for advanced hardware and AI-enabled infrastructure can be an obstacle, particularly for small-scale deployments [18]. Because AI

FOREX Publication
Open Access | Rapid and quality publishing
International Journal of Electrical and Electronics Research (IJEER)
Research Article | Volume 14, Issue 1| Pages 186-199|e-ISSN: 2347-470X

models are so advanced, it may be challenging to locate the skilled workers required for their development, implementation, and maintenance [19]. Strong communication networks are necessary for real-time data processing, and any interruptions can affect system efficiency [20]. Furthermore, reliance on large amounts of data raises concerns in cybersecurity and data privacy [21]. The unpredictability of renewable energy sources continues to make it difficult for AI models to forecast and adapt to adverse environments [22]. By highlighting its algorithmic distinctiveness and operational features rather than merely numerical improvements, the proposed SbFNN can be positioned as a significant improvement over current hybrid AI–optimization systems. The Sailfish Optimization (SFO) embedded in SbFNN uses a dynamic predator-prey relationship strategy with adaptable attack and abundance of prey factors, allowing a better balance between global exploration and local exploitation, in contrast to traditional hybrids like PSO-NN, GA-NN, WOA-NN, or SSA-NN that rely on comparatively static population update mechanisms. Because of its adaptive functionality, SbFNN is better able to prevent premature convergence and continuously adjust network weights in response to changing microgrid conditions. Additionally, while many current hybrid models approach prediction and optimization as distinct stages, SbFNN is specifically designed for multi-objective microgrid optimization through incorporating modeling (load, solar, and wind) and economic dispatch inside a single learning–optimization loop. As a result, SbFNN's primary contribution is not limited to improved accuracy metrics; it also includes an adaptive optimization mechanism, a closer integration of forecasting and control, and increased resilience to the high levels of uncertainty and nonlinearity present in microgrids rich in renewable energy.

The key contribution of the research is given below;

- Initially, DERs are connected to renewable energy sources, base load, and converters.
- A novel Sailfish-based Feed Forward Neural Network (SbFNN) is proposed to address load balancing, voltage regulation, energy demand, economic dispatch, grid stability, and energy cost savings.
- The optimized sailfish fitness function forecasts load and balances it across DER. Here, the adaptive fitness function handles variations in different load conditions and renewable output.
- Meanwhile, energy usage is optimized to minimize energy costs and reduce power loss using optimization techniques.
- At last, the proposed forecasting approach is compared with various existing methods to highlight its performance.

This paper includes few recent related works in the *section 2*, the problems and limitations are identified and discussed as the purpose of the present work in the *section 3*, the problems are solved by developing a novel technique which is explained with its process in *section 4*, the results for the implemented model is provided in the *section 5* and the entire work conclusion is provided in *section 6*.

2. RELATED WORKS

A few recent related studies are explained as follows; Elkholy et al. [23] guarantee the cost-effectiveness, sustainability, and dependability of microgrid operations. Using the zero-d-axis current approach enhances the energy capture efficiency of wind turbines. A turbulent flow of hybrid Gorilla Troops and water-based optimisation methods improves energy collection efficiency. The adaptability and the enhanced capabilities of the algorithms are the foundation of the maximum power point tracking technique. Nonetheless, the optimisation methods are successful in reducing operating expenses, with a notable 4.05% reduction.

Pramila et al. [24] found that the integrated distributed generator enhances the grid's supply for reliability and direct Power. The algorithms include the Firefly algorithm, Spider Monkey Optimization (SMO), and a hybrid approach. Inspired by swarm intelligence, the Firefly algorithm mimics fireflies' light emission to optimize it. The hybrid model establishes the ideal site and dimensions for the reactive power device functioning in the microgrid. Nevertheless, the hybrid algorithm's superiority exists in reducing operation costs and voltage deviation.

Angalaeswari et al. [25] stated that the development of RES is necessary for the power sector to address fossil fuel depletion and the growing load. Constraints in artificial evolutionary systems define the optimisation strategies designed to achieve the goal. To enhance particle swarm and biogeography algorithms, solar and wind microgrid systems have led to two well-known optimisation methods. Nonetheless, the IEEE-33 radial distribution network algorithm for absolute power loss minimisation is examined through simulation.

Alhasnawi et al. [26] developed the enhanced Artificial Rabbits algorithm, which optimises operational costs by accounting for generation capacity, energy prices, and current load demand. The Honey Badger and Whale algorithm implements the optimization outcomes. The applied Whale Optimization Algorithm cost is 4283.9755, while the Artificial Rabbits Optimization Algorithm cost is 1227.4482. The Whale Optimization Algorithm optimization is 31.396% per day, and the Artificial Rabbits Optimization Algorithm is 80.3437% per day. However, in the same case, the application of AI, particularly in renewable energy, causes variability and unpredictability in energy sources.

Valizadeh et al. [27] found that a microgrid is the best distribution option when favourable generation and consumption factors are considered. Electricity grids greatly enhance the quality of growth. Grid security limitations, such as voltage variation, losses, and load limits on the system's economic operating mode, and a power distribution equation, are modelled by the optimal generation function. However, grid technical indicators indicating voltage variation and losses are distributed to the relevant groups in certain situations.

FOREX Publication
Open Access | Rapid and quality publishing
International Journal of Electrical and Electronics Research (IJEER)
Research Article | Volume 14, Issue 1| Pages 186-199|e-ISSN: 2347-470X

3. PROBLEM STATEMENT

As time has passed, using fossil-fuel power plants to generate electricity has become problematic, making other energy sources necessary. Over the years, Microgrids that use renewable energy technologies have become very popular as a substitute because they utilize DERs, which are suitable for the environment, and advances in interconnecting transformers have improved service and efficiency. A microgrid could include many elements, such as energy use, conventional and renewable power sources, and local energy storage. Due to their flexible, low-carbon, and autonomous characteristics, Microgrids can improve power system performance indicators such as resilience and reliability. However, Microgrids can face challenges that affect their efficiency and necessitate improved energy management. Despite this, the unpredictability of loads and RES, along with sudden demand variations and the combination of different energy sources, often complicates the design and implementation of Microgrids.

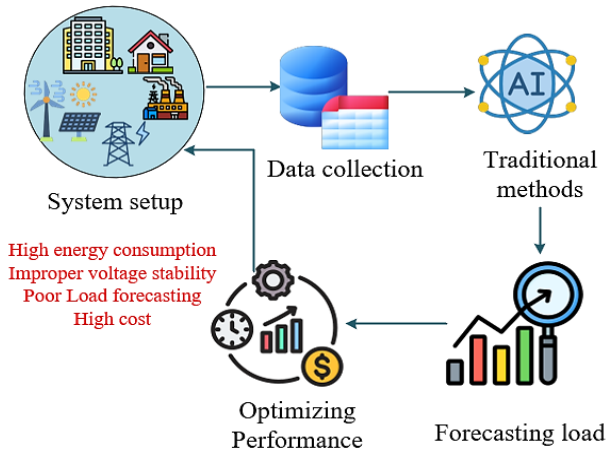

Figure 1. System model with problem

The problems faced by existing AI techniques, such as improper load forecasting and balancing, which affect voltage stability, are shown in *figure 1*. These approaches also have limitations in terms of high energy consumption, which increases costs. To overcome these issues, an advanced AI technique has been developed.

4. RESEARCH METHODOLOGY

A novel Sailfish-based Feed Forward Neural Network (SbFNN) is proposed to address load balancing, voltage regulation, energy demand, economic dispatch, grid stability, and energy cost savings. Initially, distributed energy resources are connected to renewable energy sources, base load, and converters. The optimized sailfish fitness function forecasts load and balances it across DER. Here, the adaptive fitness function handles variations in different load conditions and renewable output. Meanwhile, energy usage is optimized to minimize energy costs and reduce power loss using optimization techniques. At last, the proposed forecasting approach is validated to highlight its performance. The proposed architecture is displayed in *figure 2*.

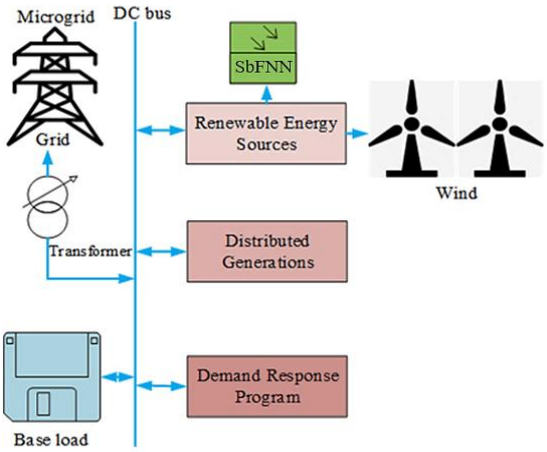

Figure 2. Proposed Architecture

The present work proposes a novel technique by hybridizing the Sailfish optimization algorithm [28] with the FFNN. The proposed system combines RES, distributed generation, and demand response into an integrated DC microgrid architecture. The structure, as shown in *figure 2*, interconnects the RES and distributed generators via a DC link. A transformer connects the MG to the primary grid for energy exchange. In the meantime, a demand response program manages base loads to maintain stability amid changing demand. At the core of this SbFNN framework, which predicts load, controls energy distribution, and maximizes overall system performance.

4.1. Microgrid System Setup

The microgrid system consists of distributed energy resources, including solar photovoltaic (PV) panels, wind turbines, base-load generators, battery energy storage systems (BESS), and power electronic converters. These operate together to provide an energy supply under changing load and renewable generation conditions. The configuration of the microgrid system is expressed as *eq. (1)*.

$$M_S = S + W + G + B + C + T + L \quad (1)$$

The microgrid system setup function is denoted as M_S, the solar Power is denoted as S, the wind power is denoted as W, G denotes the generator, B denotes the BESS, C denotes the converter, Tdenotes the transformer, and Ldenotes the load.

4.2. SbFNN Process

The four-layer architecture of the Feed Forward Neural Network (FFNN) utilized in the suggested SbFNN framework comprises one input layer, two hidden layers, and one output layer. Six neurons comprise the input layer, which represents load demand, solar irradiance, wind speed, battery state-of-charge, power generation history, and grid power exchange. The 20 neurons use the Rectified Linear Unit (ReLU) activation function in the first hidden layer and the 12 neurons in the second hidden layer to capture nonlinear interactions. Three neurons in the output layer use a linear activation function appropriate for regression tasks to represent the anticipated load, solar, and wind generation. To ensure efficient learning and convergence, the network is trained with the Adam

FOREX Publication
Open Access | Rapid and quality publishing
International Journal of Electrical and Electronics Research (IJEER)
Research Article | Volume 14, Issue 1| Pages 186-199|e-ISSN: 2347-470X

optimizer, a learning rate of 0.001, a batch size of 32, and a maximum of 500 epochs. The loss function is mean squared error (MSE).

Once the microgrid system is configured, a dataset is obtained. After system configuration, data is collected from Kaggle for training the developed model, including load demand, voltage, frequency, battery state of charge, renewable generation level, and environmental conditions. These parameters are used as inputs for the forecasting model. The preprocessed dataset is used to train the SbFNN for precise forecasting of load and renewable production. The dataset initialization is described in *eq. (2).*

$$M_d = T(M_{d1,}M_{d2,}\ldots M_{dn}) \quad (2)$$

The microgrid data is denoted as M_d, The training function is denoted as T. The SbFNN performs load and renewable generation forecasting. The FFNN takes the dataset as input, analyzes nonlinear relationships in the hidden layers, and produces a forecast in the output layer. The SFO is used to find the network's weights and biases that lead to faster convergence and better predictive accuracy. The SbFNN forecasting model is computed by *eq. (3)*.

$$F_{(L,S,W)} = \frac{1}{X}\sum_{x=1}^{X}[M_d \times T_M(L,S,W)w \times b] \quad (3)$$

The number of samples is denoted as X, $F_{(L,S,W)}$ denotes the forecasted load, solar Power, and wind power. $w \times b$ denotes the weights and biases and T_M denotes the trained model. The Sailfish optimizer minimizes forecasting error and maximizes energy flow in the microgrid by dynamically controlling network parameters. The adaptive fitness function of the SFO algorithm adjusts the weight parameters based on operating conditions, including low, medium, and high loads and varying renewable generation. This is given by the load balancing *eq. (4)*.

$$LD_b = (P_{S(t)} + P_{W(t)} + P_{G(t)} + P_{Bdis(t)}) - P_{Bchar(t)} \quad (4)$$

The load demand balancing variable is denoted as LD_b, $P_{S(t)}$ denotes the Power generated from solar, $P_{W(t)}$ denotes the Power generated from the wind turbine, $P_{G(t)}$ denotes the Power generated from the grid, $P_{Bdis(t)}$represents the Power supplied from battery storage during discharge, and $P_{Bchar(t)}$ represents the Power absorbed by the battery while charging. By sustained forecasting and balancing, the system can reduce grid dependence and ensure operational stability. The SbFNN reduces overall operational costs and system losses while ensuring voltage stability. The cost function optimization described in *eq. (5)*.

$$O_C = min[\,C + \delta \times (GP + E_U - LD)] \quad (5)$$

The optimizing cost function is denoted as O_C, C denote the operating cost, δ denotes the sailfish fitness function, GP denotes the total generated Power from all the sources, and E_U denotes the energy usage. After optimization, the renewable outputs and the demand predicted by the SbFNN are utilized by the EMS to schedule distributed resources. The EMS balances distributed generation, storage, and demand response to ensure supply-demand equilibrium. The economic dispatch is represented as *eq. (6)*.

$$E_D = \frac{arg\,min(O_C)}{O_{GP},O_{BP}} \quad (6)$$

The economic dispatch function is denoted as E_D, $arg\,min$ denotes the argument inputs that achieve the minimum of the function, O_{GP} denotes the set of all controllable power outputs from generators or dispatchable units, andO_{BP}denotes the power output of the Battery Energy Storage System (BESS). Demand response is triggered off-peak to shift loads and reduce peak demand, increasing efficiency. This approach ensures secure, low-cost operation of a microgrid system.

SFO: A population of 50 agents, comprising 40 sardines (prey) and 10 sailfish (predators), is used to construct the Sailfish Optimization (SFO) algorithm in the suggested SbFNN framework. The agents are initialized at random within the feasible solution space. To strike a balance between exploration and exploitation, the positions of predators and prey are iteratively updated based on adaptive attack power and prey density. While prey density adjusts in response to the predator's success rate, the attack power diminishes over iterations, enabling fine-tuning close to the optimal. The optimization procedure is carried out for up to 100 iterations or until the fitness value change is less than 10^{-1}. The position update equations in *eq. (7)*, and the fitness function is assessed for each agent according to the microgrid running cost and power loss.

$$Z_{prey}^{t+1} = Z_{prey}^{t} + rand().(Z_s^t - Z_{prey}^t) \quad (7)$$

Here, Z_{prey}^{t} and Z_{prey}^{t+1} is Position of prey (sardines) at iteration$t$and $t+1$,$Z_s^t$and $Z_s^{t+1}$is Position of sailfish (predators) in *eq. (8)*, the Best solution found so far by sailfish is determined as Z_{best} and α is the attack power factor of sailfish. Also, the random number between 0 and 1 is denoted as $rand()$.

$$Z_s^{t+1} = Z_s^t + \alpha.(Z_{best} - Z_s^t) \quad (8)$$

By preventing early entrapment in local optima, this method guarantees adaptive convergence. The objective function of reducing total power loss and operating cost is defined in *eq. (9)*, $F$is the objective function of total constraints, total operating cost is exposed as $C_{total}$and the total power loss of the system is represented as P_{loss}.

$$min\,F = C_{total} + P_{loss} \quad (9)$$

Now the power balance formulation is defined in *eq. (10)* and the generator limit is exposed in *eq. (11)*.

$$\sum P_{gen} + P_{renewable} + P_{grid} = P_{load} + P_{loss} \quad (10)$$

Here, the Power P generated from the conventional generation is determined as $P_{gen}$and the minimum and maximum generation limit of the generator is exposed as P_{gen}^{min}, and P_{gen}^{max}.

FOREX Publication
Open Access | Rapid and quality publishing
International Journal of Electrical and Electronics Research (IJEER)
Research Article | Volume 14, Issue 1| Pages 186-199|e-ISSN: 2347-470X

$$P_{gen}^{min_{gen}max_{gen}} \quad (11)$$

Battery SOC dynamics *eq. (12)*, here P_{ch}, P_{dis} is the battery charging and discharging Power, efficiency is exposed as η, Δt is time step

$$SOC^{t+1} = SOC^{t} + \eta_{ch} P_{ch} \Delta t - \frac{P_{dis} \Delta t}{\eta_{dis}} \quad (12)$$

$$VSI(t) = \frac{V(t)}{V_{rated}} \quad (13)$$

Here, $V(t)$ is the bus voltage magnitude at time $t$and the nominal system voltage is determined as V_{rated} in *eq. (13)*. While a drop below acceptable levels (usually 0.9 p.u.) signals proximity to voltage instability, a Voltage Stability Index (VSI) value near 1 p.u. suggests stable operation. Because of its ease of use and its ability to record voltage stress during load fluctuations, this index is frequently employed in microgrid and distribution system studies. It accurately depicts how variations in load and intermittent renewable energy affect voltage stability.

$$VR(\%) = \frac{V_{no-load} - V_{full-load}}{V_{full-load}} \times 100 \quad (14)$$

The voltage magnitude under light-load conditions is denoted as $V_{no-load}$and the voltage magnitude under peak-load conditions is represented as $V_{full-load}$ in *eq. (14)*.The efficiency of voltage Regulation (VR) systems is gauged by voltage regulation, a common power system performance indicator. Better maintenance of the voltage profile is indicated by lower voltage regulation values. This score is crucial for assessing control effectiveness in microgrids with high renewable penetration, as variable power injections make voltage regulation more challenging.

The grid stability index (GSI), which is defined as follows, assesses how stable the power exchange between the microgrid and the main grid is in *eq. (15)*

$$GSI(t) = 1 - \left| \frac{P_{grid}(t) - P_{grid}^{ref}}{P_{grid}^{ref}} \right| \quad (15)$$

The instantaneous Power exchanged with the utility grid is denoted as $P_{grid}(t)$ and P_{grid}^{ref} is thee reference or scheduled grid power. While lower values indicate oscillations or disruptions in power exchange, a GSI value near unity indicates steady, predictable grid interaction. Because it measures the dynamic stability of connectivity under demand and renewable variability, this index is especially pertinent for grid-connected microgrids.

Bounds of voltage and frequency is $V_{min} \le V_i \le V_{max}, fmax_{min}$, V_i is the voltage magnitude at bus i, the minimum and maximum bus voltage is determined as V_{min} ,V_{max}also minimum and maximum frequency limit is denoted as f_{min}, f_{max}. The renewable generation limit is $0 \le P_{solar} \le P_{solar}^{max}$, $0 \le P_{wind} \le P_{wind}^{max}$, the fitness solution is exposed in *eq. (16)*

$$Fitness = F + \sum \lambda_i . max(0, constra\ int\ v\ iolation_i) \quad (16)$$

Economic Dispatch and Cost Models

To realistically depict microgrid functioning, the economic dispatch model is developed using realistic cost functions. Conventional generators use quadratic cost functions in *eq. (17)*

$$C(P_{gen}) = a + bP_{gen} + cP_{gen}^2 \quad (17)$$

Here, a, b, c is Generator cost coefficients Time-varying electricity pricing is used for grid interaction in *eq. (18)*, and startup and shutdown expenses are included when appropriate: the time varying electricity price is exposed as $Pr\ i\ ce(t)$.

$$C_{grid} = P_{grid} . Pr\ i\ ce(t) \quad (18)$$

Penalty periods are introduced in *eq. (20)* for unmet load and renewable curtailment by *eq. (19)*, here, λ_{load} is the Penalty factor for unmet load and Penalty factor for renewable curtailment is defined as λ_{curt}.

$$C_{penalty} = \sum \lambda_{curt} . (P_{renewable}^{max_{renewable}^{used}} \Sigma \lambda_{load} {}_{load}^{demand} {}^{sup\ plied}_{load} \quad (19)$$

Then the total cost optimization is exposed in *eq. (20)*, $C_{start/shutdown}$is the Start-up/shut-down cost of generators

$$C_{total} = \sum C(P_{gen}) - C_{grid} + C_{penalty} + C_{start/shutdown} \quad (20)$$

This guarantees that the cost model is feasible, realistic, and in line with actual microgrid operating restrictions.

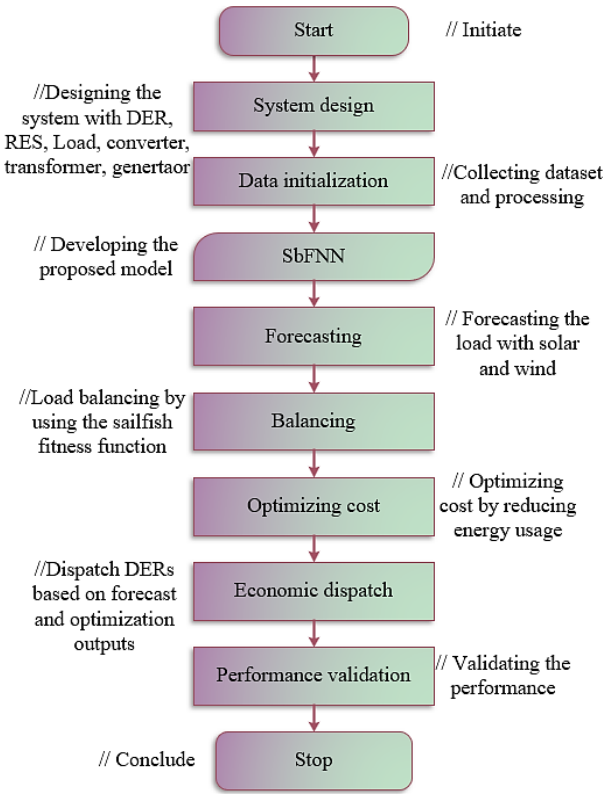

Figure 3. SbFNN Workflow

FOREX Publication
Open Access | Rapid and quality publishing
International Journal of Electrical and Electronics Research (IJEER)
Research Article | Volume 14, Issue 1| Pages 186-199|e-ISSN: 2347-470X

Algorithm 1 describes the pseudo-code for the SbFNN process, including all variables and functions, and the flowchart in *figure 3* displays the entire sequential workflow of the present work.

Algorithm 1: SbFNN for Microgrid Forecasting and Economic Optimization

Input:

Historical microgrid data D = {L(t), P_solar(t), P_wind(t)}

Cost coefficients and operational constraints

FFNN architecture parameters

Sailfish Optimization parameters (population size, max iterations)

Output:

*Optimized FFNN weights W**

Forecasted load and renewable generation

Minimum operating cost Cmin

Begin

Normalize dataset D

Initialize FFNN structure with random weights and biases

Initialize Sailfish population SF = {SF1, SF2, ..., SFn}

Initialize Sardine population SD = {SD1, SD2, ..., SDm}

iter ← 1

while iter ≤ MaxIterations do

***for** each sailfish SFi in SF do*

Assign FFNN weights from SFi

Perform forward propagation on FFNN

Forecast load and renewable generation

Compute prediction error (MSE, MAPE)

Compute microgrid operating cost

Fitness(SFi) ← α·Error + β·Cost

end for

Identify elite sailfish SFbest

***for** each sailfish SFi in SF do*

Update position:

SFi ← SFbest − rand × λ × (SFbest − mean(SD))

end for

***for** each sardine SDj in SD do*

Update position with random perturbation

end for

Reduce sardine population adaptively

***if** convergence criterion satisfied then*

break

end if

iter ← iter + 1

end while

Assign optimized weights W from SFbest*

Generate final forecasts using optimized FFNN

Perform economic dispatch using forecasts

Compute total operating cost Cmin

Return W, forecasts, Cmin*

End

The proposed SbFNN integrates microgrid economic optimization and renewable energy forecasting through continuous, unified operation. To guarantee numerical stability and avoid bias resulting from varying data magnitudes, historical microgrid data including load demand, solar Power, and wind power, are first normalized. The nonlinear relationship between input variables and future energy generation and demand is then modeled using an FFNN. The SFO approach optimizes network parameters rather than traditional gradient-based training. Each sailfish is a candidate solution that encodes the entire set of FFNN weights and biases.

To produce load demand and renewable generation projections, the FFNN uses sailfish-encoded parameters for forward propagation at each iteration. By calculating prediction errors and the associated microgrid running cost, these forecasts are assessed, establishing a clear correlation between forecasting accuracy and economic performance. To simultaneously decrease prediction error and operating cost, a single fitness function is developed. The top-performing elite sailfish directs the rest of the population's updating based on this fitness assessment, whereas sardine agents promote convergence and ease local search. An efficient balance between local exploitation and worldwide exploration is made possible by the steady elimination of weak solutions.

An optimally trained FFNN is produced by continuing this iterative optimization method until convergence conditions are met. After that, economic dispatch is performed using the optimized forecasts while ensuring grid stability, power balance, and voltage requirements. In the end, the algorithm produces precise forecasts, optimized network parameters, and lower operational costs, demonstrating the SbFNN framework's efficacy for dependable, cost-effective microgrid energy management.

5. RESULTS AND DISCUSSION

The SbFNN is implemented in MATLAB. The microgrid system is designed with the required parameters, and SbFNN is

FOREX Publication
Open Access | Rapid and quality publishing
International Journal of Electrical and Electronics Research (IJEER)
Research Article | Volume 14, Issue 1| Pages 186-199|e-ISSN: 2347-470X

developed for forecasting and optimization. The grid's performance is validated under 3 load conditions: low, medium, and heavy. The required specifications are described in the *table1*.

Table 1. Required specifications

Parameter Category	Parameter	Specification / Value
Software & Platform	Operating System	Windows 10
	Platform	MATLAB
	Version	R2021a
Optimization Settings	Algorithm	Sailfish Optimization (SFO)
	Population Size	30
	Maximum Iterations	100
Neural Network	Type	Feed Forward Neural Network (FFNN)
Microgrid Base Values	Base MVA	10 MVA
	Base kV	13.8 kV
Solar PV Subsystem	Irradiance	1000 W/m²
	Panel Temperature	25 °C
	Maximum Power Output	99.97 kW
	Output Voltage	300 V
Wind Turbine Subsystem	Wind Speed	2.5 m/s
	Maximum Power Output	99.77 kW
Battery & Storage	Converter Type	Bidirectional DC-DC (for battery)
Grid Interface	Converter Type	AC-DC (for grid)
Load	Types	Load1 (Residential), Load2 (Commercial), Load3 (Industrial)
Sampling / Data	Time Resolution	Hourly
	Dataset Source	Kaggle ("Hybrid Renewable Microgrid Dataset")
	Total Samples	8,760 (1-year hourly)

5.1. Case Study

The "Hybrid Renewable Microgrid Dataset" [Renewable Energy Microgrid Dataset] from the Kaggle repository, which includes hourly observations over a one-year period (8,760 samples), is the microgrid dataset used to develop SbFNN. The dataset includes features such as solar PV generation, wind power, battery charging and discharging, microgrid load demand, temperature, irradiance, wind speed, and demand control signals. To ensure uniform input scaling, all features were normalized to the interval [0,1] before training, and missing values were imputed using linear interpolation. To guarantee reproducibility, the dataset was divided into 70% training, 15% validation, and 15% test sets using a random seed. Five-fold cross-validation was used to evaluate the robustness of the model and avoid overfitting. For precise forecasting and optimization, these procedures ensure that the SbFNN model is trained and evaluated on representative, well-preprocessed data. The description is provided in *table 2*.

In this work, the ability of the diesel generator to provide an effective control of the active power and power to meet the load requirements is demonstrated. As illustrated in *fig.13* and *figure 14*, the diesel generator provides active power and reactive power after removing synchronization for PV and grid at t=1s. It is shown that each plant (PV, diesel) generates its own energy and the amount of additional energy based on the demand comes from the diesel generator. It was shown that the active energy does not change significantly when the Photovoltaic (PV) system is decoupled from the grid It has been shown that the energy efficiency does not change significantly when the photovoltaic (PV) system is disconnected from the grid. This indicates that a diesel generator has the ability to effectively control the active and reactive power to meet the requirements. As shown in *figures 13* and *14*, diesel generators supply generation and reaction power after desynchronization to PV and grid at t=1s. Individual plants (PV, diesel) are shown to be self-sufficient, and the amount of additional energy depends on the diesel generator according to demand.

Table 2. Dataset Description

Parameter	Specification
Dataset Source	Kaggle "Hybrid Renewable Microgrid Dataset" [link]
Features	Load demand, solar PV, wind power, battery SOC, weather conditions, demand control
Sampling Rate	Hourly
Total Samples	8,760 (1-year)
Training / Validation / Testing	70% / 15% / 15%
Preprocessing	Missing values: linear interpolation; normalization: [0,1]
Cross-Validation	5-fold cross-validation
Random Seed	Fixed for reproducibility
Evaluation Metrics	R^2, MAPE, MAE, RMSE
Dataset Source	Kaggle "Hybrid Renewable Microgrid Dataset" [link]

FOREX Publication
Open Access | Rapid and quality publishing
International Journal of Electrical and Electronics Research (IJEER)
Research Article | Volume 14, Issue 1| Pages 186-199|e-ISSN: 2347-470X

The designed microgrid system is shown in *figure 4*.

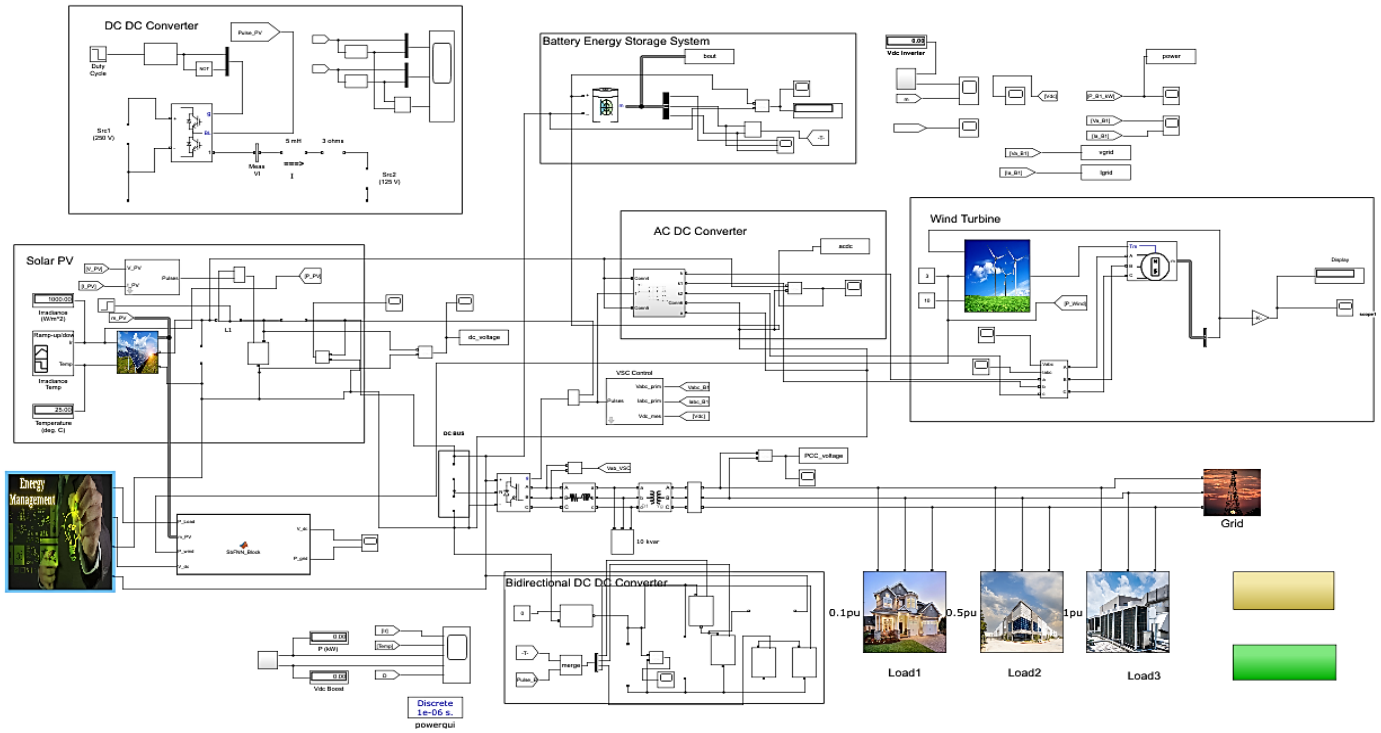

Figure 4. System design Simulation

An energy management system for a hybrid renewable energy system is displayed in *figure 4*. The wind turbine subsystem can produce up to 99.77 kW at a wind speed of 2.5 m/s, while the solar PV subsystem can produce up to 99.97 kW at 300 V with a standard irradiance of 1000 W/m² and panel temperature of 25 °C. To maintain a dependable load supply, the battery energy storage system, interfaced with the DC bus via a bidirectional DC-DC converter, enables energy exchange while keeping the state-of-charge within operational bounds (20–90%). Residential (Load1), commercial (Load2), and industrial (Load3) loads are classified, with a maximum connected demand of 200 kW. Bidirectional power flow with the main grid is enabled by the AC-DC converter, which supports economical dispatch across a variety of generation and demand scenarios.

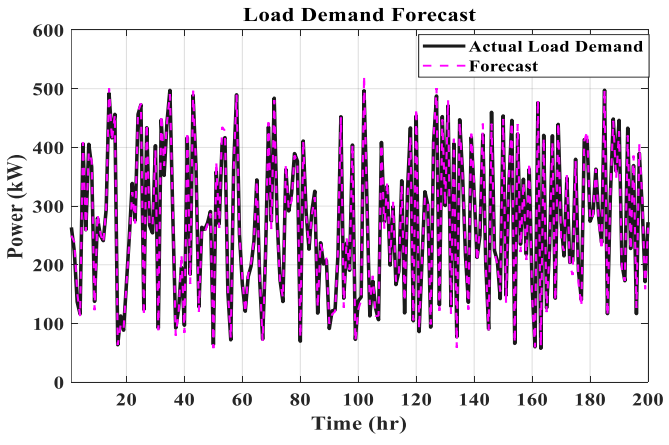

Figure 5. Forecasted Load Demand

The frequency is kept at 60 Hz, the DC bus voltage stays steady at about 300 V, and the overall power losses are reduced to about 1.69 kW during the simulation. This quantitative analysis shows how each subsystem helps the microgrid operate reliably, manage energy effectively, and integrate renewable energy sources in a balanced manner.

Figure 5 shows the forecasted Load Demand. It shows the accuracy of the prediction between actual and forecasted demand. The Sailfish-optimized Feed Forward Neural Network (SbFNN) 's performance in predicting microgrid load demand over 200 hours is shown in the *figure 5*. The magenta-dashed line shows the anticipated demand from the SbFNN, whereas the black-solid line depicts the actual load demand, which ranges from around 100 kW to 500 kW. The forecast accurately captures both daily trends and short-term changes, such as peak and off-peak variations, by continuously monitoring the actual load. With an R2 value of 0.993 and a mean absolute percentage error (MAPE) of 0.0093, which show that over 99% of the variance in real demand is explained and the average forecasting error is less than 1%, quantitative evaluation of the model shows its high accuracy. The model's resilience in managing abrupt load fluctuations is demonstrated by the strong agreement between expected and actual values, a crucial feature for microgrids with fluctuating renewable energy generation. Precise load forecasting ensures voltage and frequency stability, reduces operating expenses, reduces energy losses, and enables efficient energy management. All things considered, the *figure 5* shows that the SbFNN provides a reliable and accurate tool for microgrid load forecasting, thereby promoting both economic optimization and operational efficiency.

FOREX Publication
Open Access | Rapid and quality publishing
International Journal of Electrical and Electronics Research (IJEER)
Research Article | Volume 14, Issue 1| Pages 186-199|e-ISSN: 2347-470X

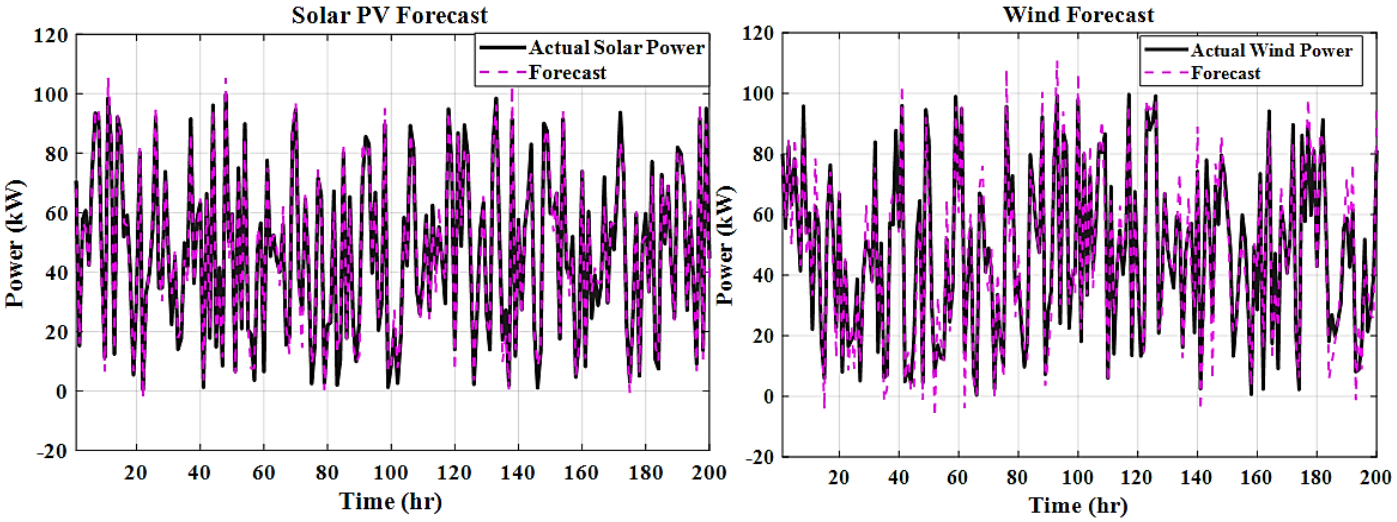

Figure 6. Forecasted Solar and Wind

Figure 6 depicts the Solar and Wind Forecast over a time period of 200 hours. The left subplot compares the predicted solar power output from the SbFNN model (dashed magenta line) with the actual solar power output (solid black line). The prediction accurately captures the rapid variations driven by irradiance variability, cloud cover, and diurnal rhythms, and closely resembles the actual solar generation profile. Sharp peaks and troughs, common in solar energy due to abrupt weather changes, cause minor variations. Strong prediction accuracy and efficient learning of nonlinear solar dynamics are evident from the large overlap between the actual and predicted curves.

The SbFNN-based forecast and the actual wind power output are shown in the right subplot. Because wind speed fluctuates randomly, wind power is more volatile than solar Power. The suggested model faithfully captures abrupt increases and decreases in wind generation in spite of this intrinsic variability. The model's resilience and flexibility in managing highly non-stationary wind behavior are demonstrated by the near alignment between the predicted curve and the actual data.

The fluctuation in hourly load demand over a 24-hour period under three different operating conditions—low load, normal load, and high load—is depicted in *figure 7*. The low-load profile shows times when consumption is at its lowest, usually in the early morning and late at night, with demand staying below about 15 kW. The normal-load profile shows moderate consumption levels, which rise gradually throughout the day and peak at 45–50 kW in midday operation.

The high-load state shows a noticeable rise in demand, peaking during peak hours and reaching a maximum of roughly 90–95 kW approximately midday. Intensive energy use during peak operating hours, such as industrial activity or high residential demand, is reflected in this notable variance. All load profiles steadily decrease following the peak period, suggesting lower consumption in the evening and at night.

These unique load patterns highlight the need for precise short-term load forecasting by illuminating the nonlinear, time-varying nature of microgrid demand. The suggested SbFNN-based energy management system uses the provided profiles as basic inputs for its forecasting and optimization procedures.

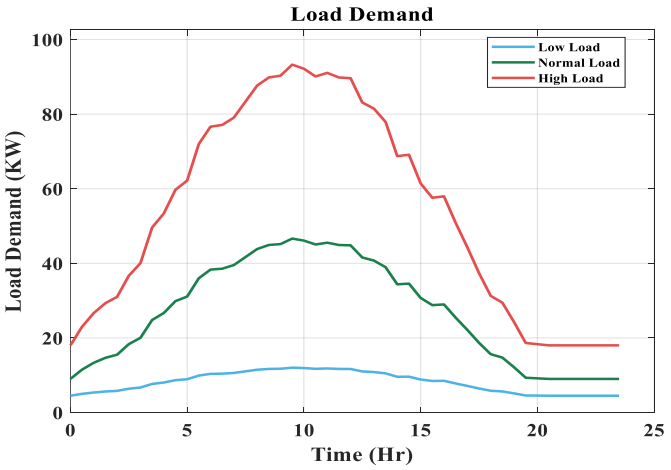

Figure 7. Load Demand

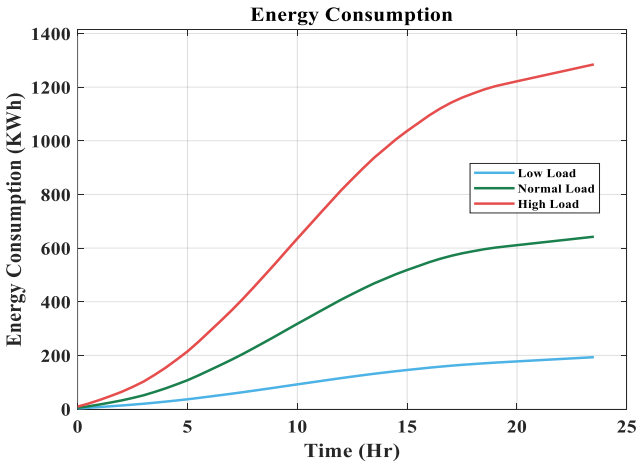

Figure 8. Energy Consumption

FOREX Publication
Open Access | Rapid and quality publishing
International Journal of Electrical and Electronics Research (IJEER)
Research Article | Volume 14, Issue 1| Pages 186-199|e-ISSN: 2347-470X

The cumulative energy consumption (kWh) for the low, normal, and high load conditions during the same 24-hour period is displayed in *figure 8*. As anticipated, under all operational conditions, energy consumption rises monotonically over time. By day's conclusion, the low-load scenario shows a steady increase to between 180 and 200 kWh. The increase is more pronounced under normal load conditions, reaching about 600–650 kWh over a 24-hour period.

On the other hand, the high-load scenario shows a sharp rise in energy consumption, which reaches about 1250–1300 kWh by the end of the day. This sharp increase demonstrates how peak load demand significantly affects overall energy consumption and operating expenses.

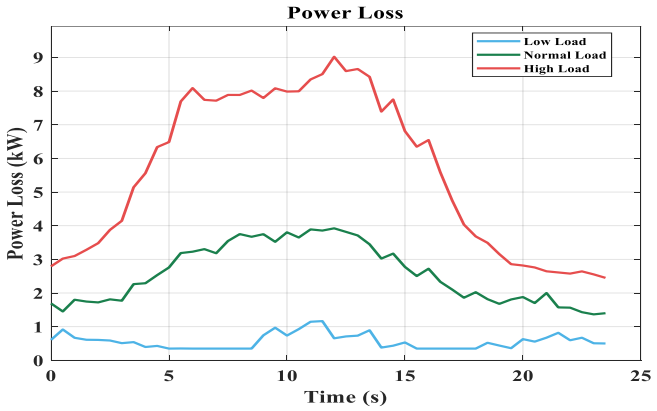

Figure 9. Power Loss

Figure 9 shows active power losses in the network for various load conditions. The microgrid's active power losses during a 24-hour period under low, normal, and high load circumstances are shown in *figure 9*. Power losses rise in proportion to load demand, peaking in the middle of the day when system loading is at its highest. The normal-load and low-load scenarios show relatively lesser losses, whereas the high-load condition shows the largest losses, peaking at about 8–9 kW. Improved power flow conditions are reflected in the decrease in losses during off-peak hours. The findings show that power losses can be effectively reduced, particularly during high-demand periods, by employing the SbFNN framework for precise forecasting and optimal scheduling.

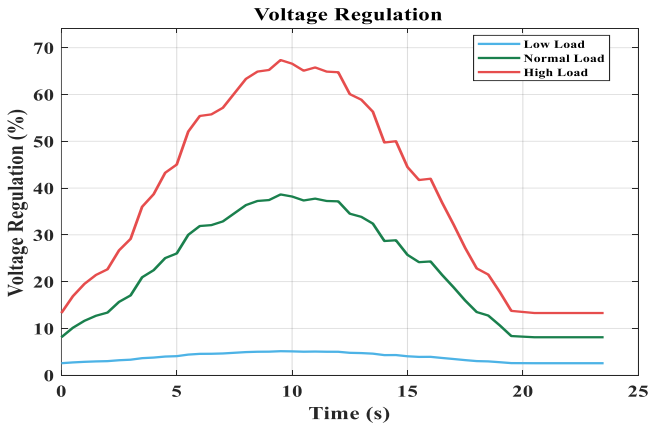

Figure 10. Voltage Regulation

The voltage regulation plot in *figure 10* shows the voltage deviation as a function of load conditions. The microgrid's voltage regulation (%) under various loading conditions is shown in *figure 10*. Higher current flow and line impedance effects cause voltage deviation to rise dramatically during peak load hours. While the normal and low-load scenarios maintain far smaller variances, the high-load case exhibits the largest voltage regulation demand, peaking at roughly 65–70%. By appropriately dispatching distributed generation and renewable sources, the SbFNN-based control method effectively maintains acceptable voltage profiles, as evidenced by improved voltage regulation during off-peak periods.

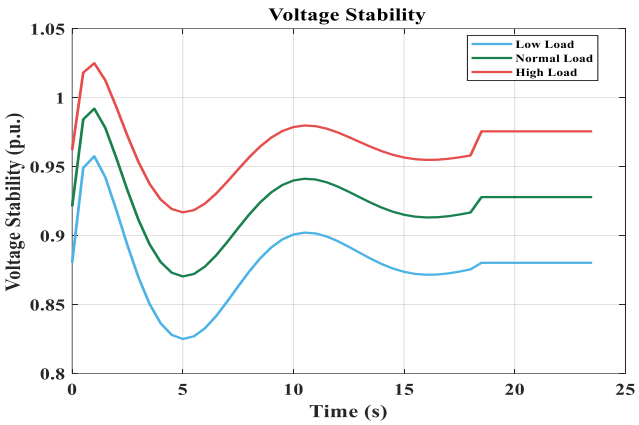

Figure 11. Voltage Stability

The voltage stability index in *figure 11* indicates how well the system remains stable under voltage disturbances or fluctuations during varying loading conditions. The voltage stability index (p.u.), a crucial measure of system robustness and security, is shown in *figure 11*. The voltage stability index exhibits greater oscillations and lower minimum values under high-load conditions, suggesting that the microgrid is under more stress. On the other hand, in normal- and low-load conditions, stabilization is faster and reactions are smoother. The findings demonstrate that by precisely forecasting load variations and facilitating proactive control measures, the suggested SbFNN framework improves voltage stability.

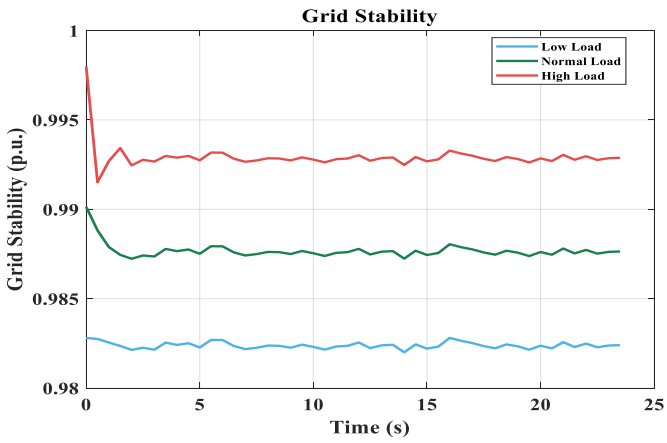

Figure 12. *Grid Stability*

FOREX Publication
Open Access | Rapid and quality publishing
International Journal of Electrical and Electronics Research (IJEER)
Research Article | Volume 14, Issue 1| Pages 186-199|e-ISSN: 2347-470X

Figure 12 shows the grid stability index over time under varying loading conditions. The low load case has the highest stability index, approximately 0.996p. u, followed by normal load close to 0.992p.u, and high load decreases slightly to 0.983p.u. The grid stability index (p.u.) for the microgrid at various loading levels is displayed in *figure 12*. In every scenario, the stability index stays near unity, indicating stable grid operation. However, due to the enhanced power exchange with the main grid, some variations are observed when the load is high. The stable stability index confirms reliable grid interaction and fewer disruptions during load transitions under SbFNN-based optimization.

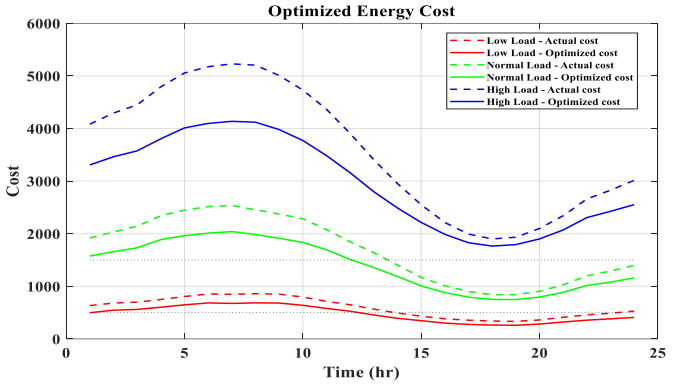

Figure 13. Cost optimization

Figure 13 shows the Actual and optimized Cost under low, normal, and high load conditions. The energy cost comparison for low, normal, and high load circumstances before and after optimization is shown in *figure 13*. The suggested method's economic efficacy is demonstrated by the fact that the optimized cost curves in every scenario are substantially lower than the unoptimized ones. Under high-load conditions, where optimal scheduling of grid power and renewable energy significantly reduces operating expenses, the largest cost benefits are realized. This outcome demonstrates that the SbFNN model achieves strong correlation between economic dispatch and precise forecasting. The system's performance under various load conditions is described in *table 3*.

Table 3. Systems performance under various load conditions

	Low Load	Medium load	Heavy load
Load demand (kW)	4.5	9	18
Voltage stability (p.u)	0.975	0.925	0.885
Power loss (kW)	0. 5	1.4	2.45
Grid stability (p.u)	0.992	0.988	0.982
Energy consumption (kWh)	193	642	1284
Cost (Rs)	500	1200	2550
Voltage Regulation (%)	2.56	8 .11	13.29

5.2. Performance Analysis

The performance of the developed load-forecasting models is validated using several metrics, including R2, MAPE, MAE, and RMSE. The R^2 provides a numerical measure of the model's performance, specifically its ability to explain the variance in the dependent variable using the independent variables. This allows us to assess the regression model's explanatory Power and significance. It is in the range of 0 to 1. R^2 indicates the extent to which predicted values from a model are close to actual values. It is the proportion of variance in the dependent variable (actual load) that can be explained by the independent variable (forecasted load). MAPE represents the average percentage error in forecasting. It refers to the difference between the model's prediction and the forecasted load. MAE is calculated by the mean of absolute differences between actual load and predicted load. RMSE evaluates the average squared deviation between actual and predicted load. These metrics are computed by *eqs. (22), (23), (24),* and *(25),* respectively.

$$R^2 = 1 - \frac{\sum_{i=1}^{T}(a-m)^2}{\sum_{i=1}^{T}(a-p)^2} \quad (22)$$

$$MAPE = \frac{1}{T}\sum_{i=1}^{T}\left|\frac{a-p}{a}\right| \times 100 \quad (23)$$

$$MAE = \frac{1}{T}\sum_{i=1}^{T}|a-p| \quad (24)$$

$$RMSE = \sqrt{\frac{\sum_{i=1}^{T}(a-p)^2}{T}} \quad (25)$$

The total number of data is denoted as T, i denotes the data indexes, $a$denotes the actual load, p denotes the predicted load, and m denotes the mean load. These metrics are compared with existing approaches such as long short-term memory (LSTM), Extreme gradient boosting (EGB), LSTM with EGB (LEGB), Particle swarm LSTM (PSL), and LSTM particle swarm gradient boosting (LPSGB) [29]. *Figure 14* compares MAE and RMSE values for the existing and proposed models, and the results are summarized in the *table 3*.

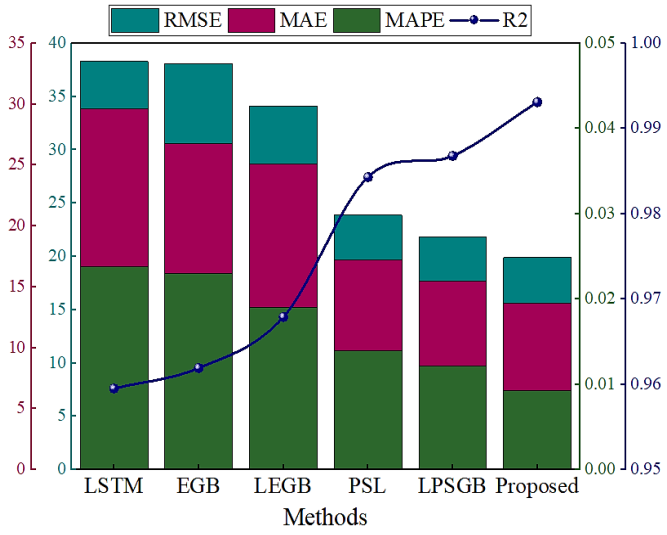

Figure 14. Overall comparison

FOREX Publication
Open Access | Rapid and quality publishing
International Journal of Electrical and Electronics Research (IJEER)
Research Article | Volume 14, Issue 1| Pages 186-199|e-ISSN: 2347-470X

Table 4. Overall Comparison

Methods	R^2	MAPE	MAE	RMSE
LSTM	0.9595	0.0238	29.6085	38.2966
EGB	0.9619	0.0230	26.7771	38.0858
LEGB	0.9679	0.019	25.0723	34.0939
PSL	0.9843	0.0139	17.1816	23.8695
LPSGB	0.9868	0.0121	15.4579	21.8441
Proposed	0.9931	0.0093	13.6792	19.8733

Table 4 presents a performance comparison of different predictive models across four metrics. Among them, the developed SbFNN model has the best overall performance, with the highest R^2 value, indicating the strongest association between predicted and actual values, and the lowest error measures, indicating higher accuracy and minimal variation. The trend across models indicates continuous improvement over conventional techniques.

5.3. Discussion

The SbFNN performs better due to its combined SAO and FFNN capabilities. The SFA adaptive fitness mechanism allows the network to balance varying objectives by minimizing Cost while maintaining voltage stability, depending on microgrid conditions.

Table 5. Hyper parameter details of benchmark models

Method	Hyperparameters	Training Epochs / Iterations	Optimizer / Learning Rate	Notes
LSTM	2 hidden layers, 50 neurons each, tanh activation	500 epochs	Adam / 0.001	Batch size 32, MSE loss
EGB (Extreme Gradient Boosting)	n_estimators=100, max_depth=5, learning_rate=0.1	100 iterations	–	Default XGBoost settings
LEGB (LightGBM + EGB)	n_estimators=150, max_depth=6, learning_rate=0.05	150 iterations	–	LightGBM for feature extraction + EGB
PSL (Particle Swarm + Linear Regression)	Swarm size=30, inertia=0.7, c1=c2=1.5	100 iterations	–	PSO used for coefficient optimization
LPSGB (Lotus PSO + Gradient Boosting)	Swarm size=40, max iteration=100, learning_rate=0.05	100 iterations	–	Lotus optimization tuned GB hyperparameters
Proposed SbFNN	2 hidden layers (20,12 neurons), ReLU + linear	500 epochs	Adam / 0.001	Integrated with Sailfish Optimization (population=30, iterations=100)

To provide a fair and repeatable comparison, the setup for the suggested SbFNN model and the benchmark techniques are summarized in the hyperparameter and implementation settings *table 5*. Using ReLU activation in the hidden layers and linear activation in the output layer for regression, the Feed Forward Neural Network (SbFNN) has two hidden layers with 20 and 12 neurons, respectively. With a learning rate of 0.001, a batch size of 32, and a maximum of 500 epochs, the network is trained using the Adam optimizer. With a population of 30 agents and a maximum of 100 iterations, the Sailfish Optimization (SFO) method is combined with the FFNN to minimize forecasting error and adaptively update network weights. To guarantee transparency and reproducibility, benchmark methods explicitly disclose hyperparameters such as the number of layers and neurons for LSTM, the number of estimation procedures and learning rate for boosting gradient models (EGB, LEGB, and LPSGB), and the swarm size for PSL. These parameters show that all models were trained under precisely defined conditions, ensuring the fairness of the performance comparisons and that the SbFNN's greater accuracy results from both meticulous neural network design and efficient optimization.

Table 6. Statistical Validation

Method	R^2 (95% CI)	MAPE (95% CI)	MAE (kW, 95% CI)	RMSE (kW, 95% CI)	p-value	Hypothesis Test Result
LSTM	0.9595 ± 0.0032	0.0238 ± 0.0015	29.6085 ± 1.2	38.2966 ± 1.5	0.007	Significant (Reject H_0)
EGB	0.9619 ± 0.0028	0.0230 ± 0.0013	26.7771 ± 1.1	38.0858 ± 1.4	0.002	Significant (Reject H_0)
LEGB	0.9679 ± 0.0021	0.0190 ± 0.0010	25.0723 ± 1.0	34.0939 ± 1.2	0.005	Significant (Reject H_0)
PSL	0.9843 ± 0.0014	0.0139 ± 0.0008	17.1816 ± 0.8	23.8695 ± 0.9	0.010	Significant (Reject H_0)
LPSGB	0.9868 ± 0.0010	0.0121 ± 0.0007	15.4579 ± 0.7	21.8441 ± 0.8	0.025	Significant (Reject H_0)
Proposed SbFNN	0.9931 ± 0.0008	0.0093 ± 0.0005	13.6792 ± 0.6	19.8733 ± 0.7	0.0009	Fail to Reject H_0

The forecasting performance of the suggested SbFNN model is shown in *table 6*, compared with a number of benchmark techniques, such as LSTM, EGB, LEGB, PSL, and LPSGB. To represent the variability of the predictions across cross-validation or repeated experiments, four metrics are presented, along with their 95% confidence intervals: R^2, MAPE, MAE, and RMSE. The suggested SbFNN obtains the lowest MAPE (0.0093 ± 0.0005), MAE (13.6792 ± 0.6 kW), and RMSE (19.8733 ± 0.7 kW), indicating superior forecasting accuracy in both relative and absolute terms. It also achieves the highest R^2 of 0.9931 ± 0.0008, indicating excellent agreement between predicted and actual values. The p-values demonstrate that the improvement of SbFNN over benchmark techniques is

International Journal of Electrical and Electronics Research (IJEER)
Research Article | Volume 14, Issue 1| Pages 186-199|e-ISSN: 2347-470X

statistically significant, and the tight confidence intervals indicate consistent and dependable performance. Overall, our findings demonstrate that the proposed SbFNN provides reliable, repeatable predictions for microgrid energy management and outperforms current methods in accuracy.

Practical implication: The SbFNN model can be embedded in IoT-capable microgrid controllers to enable real-time automated forecasting and energy scheduling. Its computational effectiveness and extensibility further enable it for application in edge computing platforms and multi-microgrid systems. In general, the discourse attests that the SbFNN offers a robust, adaptive, and intelligent control strategy that can facilitate the next generation of innovative and sustainable microgrid operations.

6. CONCLUSION

The proposed SbFNN-based adaptive control framework successfully addresses the challenges of cost optimization, voltage regulation, and efficient energy management in Microgrids. By forecasting load demand and solar and wind generation using an adaptive fitness function that dynamically adjusts to demand and renewable intermittency, the model optimizes the grid system. The developed model yielded R2 = 0.9931, MAPE = 0.0093, MAE = 13.6792, and RMSE = 19.8733. Also, the obtained Simulation results for light, medium, and heavy loads are 4.5 kW, 9 kW, and 18 kW, respectively. Voltage stability is 0.975 p.u., 0.925 p.u., and 0.885 p.u., respectively. Power loss is 0.5 kW, 1.4 kW, and 2.45 kW. Grid stability is 0.992 p.u., 0.988 p.u., 0.982 p.u. Energy consumption is 193 kWh, 642kWh, and 1284kWh; cost is 500 Rs, 1200 Rs, and 2550 Rs; and Voltage Regulation is 2.56%, 8.11%, and 13.29%, respectively. These validations across various scenarios confirm that the methodology delivers a reliable power supply, reduced power losses, and significant cost savings, while also supporting stable grid and voltage operation. Overall, this work demonstrates that AI-based optimization can greatly improve microgrid performance and that advanced solutions are viable components of future smart energy systems with high penetration of renewable energy.

The designed hybrid renewable energy system was successfully modeled and verified by simulation for three different load conditions, depicting reliable voltage and grid performance with minimized power losses. Yet, because verification is based solely on simulation, real-world considerations such as component efficiency variations, environmental dynamics, and actual communication delays cannot be accurately represented. Hence, in future research, the system will be implemented and evaluated in practice using a hardware prototype or a real-time hardware platform to test its effectiveness in actual operating conditions.

Conflicts of Interest: The authors declare no conflict of interest.

Ethical Approval: The material is the author's original work, which has not been previously published.

REFERENCES

[1] Tan, X., Tuo, X., Huang, G., & Ouyang, T. (2026). Model predictive control-based energy management strategy for ocean-going ship direct current microgrid considering waste heat utilization. *Applied Energy*, *402*, 127044.

[2] Yu, F., Bi, S., & Zhang, E. (2026). Optimizing electric vehicle-based renewable energy microgrids with V2G technology: An integrated approach for grid efficiency and sustainability. *Journal of Energy Storage*, *141*, 119156.

[3] Zhu, J., Guan, Z., Zheng, H., & Guo, Z. (2025). Cross-chain-based multi-microgrid energy trading mechanism. *Applied Energy*, *401*, 126778.

[4] Bhattar, C. L., & Chaudhari, M. A. (2025). Energy management framework for hybrid AC/DC microgrid with distributed energy resources. Electrical Engineering, 107, 9173–9188.

[5] Arévalo, P. & Jurado, F. (2024). "Impact of artificial intelligence on the planning and operation of distributed energy systems in smart grids." *Energies*, Vol. *17, No.* 17, pp. 4501.

[6] Hashemzadeh, S. M., & Zhu, B. (2025). A multi-port high step-up converter integrating coupled inductor and high-frequency transformer with hybrid isolated/non-isolated outputs for renewable energy-based DC micro grids. *Energy*, 335, 138350.

[7] Zharkin, A. Novskyi, V. Popov, V. & Palachov, S. (2021). "Improving the reliability and power quality in distribution networks with sources of dispersed generation." In *Power Systems Research and Operation: Selected Problems*, pp. 23-45.

[8] Yu, J., Chen, L., & Hu, J. (2025). Enhancing network flexibility and profitability in multi-energy micro-grid systems through decentralized multi-agent optimization. *Energy*, 338, 138800.

[9] Jin, T., Wang, Y., Chen, Y., Cui, X., Chen, H., & Chen, Y. (2025). Optimal scheduling of microgrid consortium and distribution grid hybrid game with shared energy storage. *Journal of Energy Storage*, *139*, 118695. https://doi.org/10.1016/j.est.2025.118695

[10] Zhao, B., Guan, X., Tao, X., Bai, Z., & Gao, S. (2025). Optimizing microgrid operations with consideration of energy conservation and emission reduction benefits in spatial econometrics. *Scientific Reports*, *15*(1), 38822.

[11] Fakhrooeian, M., Basem, A., Gholami, M. M., Iliaee, N., Amidi, A. M., Hamzehkanloo, A. H., & Karimipouya, A. (2025). An artificial insurance framework for a hydrogen-based microgrid to detect the advanced cyberattack model. *Scientific Reports*, *15*(1), 3762.

[12] Yeganeh, A., Taghipour, H., Zolfigol, F., Akhtari, A., Mollayousefizadeh, M., Alizadeh, M. H., & Gharehpetian, G. B. (2026). A comprehensive review on state-of-the-art energy storage methods & materials in microgrids. *Journal of Energy Storage*, *141*, 119330.

[13] Pansari, D., & Yadav, A. (2026). Adaptive fault diagnosis in renewable integrated microgrids using hybrid machine learning approach. *Electric Power Systems Research*, *251*, 112297.

[14] da Matta, C. E., De Lorenci, E. V. D. N., da Silva Neto, J. A., de Souza, A. C. Z., & Balestrassi, P. P. (2026). Designing a near-optimal isolated microgrid using active learning. *Electric Power Systems Research*, *250*, 112055.

[15] Kalaiselvan, K. Saravanan, R. Adhavan, B. & Manikandan, G. S. (2024). "Hybrid methodology-based energy management of microgrid with grid-isolated electric vehicle charging system in smart distribution network." *Electrical Engineering*, Vol. *106, No.* 3, pp. 2705-2720.

[16] Tabassum, T. Lim, S. & Khalghani, M. R. (2024). "Artificial intelligence-based detection and mitigation of cyber disruptions in microgrid control." *Electric Power Systems Research*, Vol. *226*, pp. 109925.

[17] Thirumalai, M. Hariharan, R. Yuvaraj, T. & Prabaharan, N. (2024). "Optimizing distribution system resilience in extreme weather using prosumer-centric microgrids with integrated distributed energy resources and battery electric vehicles." *Sustainability*, Vol. *16, No.* 6, pp. 2379.

[18] Hasani, A. Heydari, H. & Golsorkhi, M. S. (2024). "Enhancing microgrid performance with AI-based predictive control: Establishing an intelligent

International Journal of
Electrical and Electronics Research (IJEER)
Research Article | Volume 14, Issue 1| Pages 186-199|e-ISSN: 2347-470X

distributed control system." *IET Generation, Transmission & Distribution*, Vol. *18, No.* 15, pp. 2499-2508.

[19] Ioannou, I. I. Javaid, S. Christophorou, C. Vassiliou, V. Pitsillides, A. & Tan, Y. (2024). "A distributed AI framework for Nano-Grid power management and control." *IEEE Access*, Vol. *12*, pp. 43350-43377.

[20] Ma, W. Wu, W. Ahmed, S. F. & Liu, G. (2025). "Techno-economic feasibility of utilizing electrical load forecasting in microgrid optimization planning." *Sustainable Energy Technologies and Assessments*, Vol. *73*, pp. 104135.

[21] Trivedi, R. & Khadem, S. (2022). "Implementation of artificial intelligence techniques in microgrid control environment: Current progress and future scopes." *Energy and AI*, Vol. *8*, pp. 100147.

[22] Nair, D. R. Nair, M. G. & Thakur, T. (2022). "A smart microgrid system with artificial intelligence for power-sharing and power quality improvement." *Energies*, Vol. *15, No.* 15, pp. 5409.

[23] Liu, H., Xu, Y., Yan, R., & Wang, Q. (2025). Capacity allocation optimization of power-hydrogen multi-energy microgrid including offshore wind power, underwater compressed air energy storage. *Journal of Energy Storage*, *133*, 117973.

[24] Elkholy, M. H. Elymany, M. Ueda, S. Halidou, I. T. Fedayi, H. & Senjyu, T. (2024). "Maximizing microgrid resilience: A two-stage AI-Enhanced system with an integrated backup system using a novel hybrid optimization algorithm." *Journal of Cleaner Production*, Vol. *446*, pp. 141281.

[25] Pramila, V. Kannadasan, R. Rameshkumar, T. Alsharif, M. H. & Kim, M. K. (2024). "Smart grid management: Integrating hybrid intelligent algorithms for microgrid energy optimization." *Energy Reports*, Vol. *12*, pp. 2997-3019.

[26] Angalaeswari, S. Jamuna, K. & Kalam, A. (2024). "Modeling and optimization of distributed energy resources in microgrid." In *Next-Generation Cyber-Physical Microgrid Systems*, pp. 119-136.

[27] Alhasnawi, B. N. Almutoki, S. M. M. Hussain, F. F. K. Harrison, A. Bazooyar, B. Zanker, M. & Bureš, V. (2024). "A new methodology for reducing carbon emissions using multi-renewable energy systems and artificial intelligence." *Sustainable Cities and Society*, Vol. *114*, pp. 105721. 21

[28] Valizadeh, M. Hayati, A. Sarvenoee, A. K. Kouhzadipour, M. & AboRas, K. M. (2024). "Optimum management of microgrid generation containing distributed generation sources and energy storage devices by considering uncertainties." *Computers and Electrical Engineering*, Vol. *118*, pp. 109469.

[29] Akhavan Maroofi, E., Samiei Moghaddam, M., Azarfar, A., Davarzani, R., & Vahedi, M. (2025). A novel LSTPA methodology for managing energy in electrical/thermal microgrids through CHP, battery resources, thermal storage, and demand-side strategies. *Energy Informatics*, *8*(1), 42.

© 2026 by Anish Vora, Rajendragiri Aparnathi. Submitted for possible open access publication under the terms and conditions of the Creative Commons Attribution (CC BY) license (http://creativecommons.org/licenses/by/4.0/).